Technische Universität Graz

The All-Floating Boundary Element Tearing and Interconnecting Method

G. Of, O. Steinbach

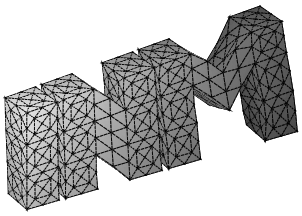

Berichte aus dem Institut für Numerische Mathematik

Bericht 2009/3

Technische Universität Graz

The All-Floating Boundary Element Tearing and Interconnecting Method

G. Of, O. Steinbach

Berichte aus dem Institut für Numerische Mathematik

Bericht 2009/3

Technische Universität Graz
Institut für Numerische Mathematik
Steyrergasse 30
A 8010 Graz

WWW: `http://www.numerik.math.tu-graz.ac.at`

The All-Floating Boundary Element Tearing and Interconnecting Method

G. Of, O. Steinbach

Institute of Computational Mathematics
Graz University of Technology
Steyrergasse 30
A-8010 Graz, Austria
{of,o.steinbach}@tugraz.at

Abstract

The all-floating Boundary Element Tearing and Interconnecting method incooperates the Dirichlet boundary conditions by additional constraints in the dual formulation of the standard Tearing and Interconnecting methods. This simplifies the implementation, as all subdomains are considered as floating subdomains. The method shows an improved asymptotic complexity compared to the standard BETI approach. The all-floating BETI method is presented for linear elasticity in this paper.

1 Introduction

Domain decomposition methods offer a comfortable treatment of coupled boundary value problems and provide efficient tools for the numerical simulation in particular by parallelization. The local subproblems can be solved by the most suitable discretization methods, e.g. finite and boundary element methods.

The Boundary Element Tearing and Interconnecting (BETI) method was introduced in [16] as the counterpart of the boundary element method to the well–known Finite Element Tearing and Interconnecting (FETI) methods [6, 7], which are widely used in engineering applications. For a detailed description of several kinds of FETI methods and a wide collection of references see the monograph [30]. The coupling of FETI and BETI methods is discussed in [17]. The main ideas of these methods are the tearing of the primal global degrees of freedom into local ones and the subsequent interconnecting of the local degrees of freedom across the interfaces by means of constraints and Lagrange multipliers as dual variables to enforce the continuity of the local variables across the interfaces. Subdomains without sufficient Dirichlet boundary conditions are called floating subdomains and

can be treated separately by using a pseudo inverse. The extra degrees of freedom related to the local rigid body motions have to be eliminated by the use of an appropriate orthogonal projection, see e.g. [2, 11]. In the case of linear elastostatics, this may become rather complicated since the number of involved rigid body motions may differ from subdomain to subdomain. The so–called FETI–DP methods [5] introduce primal variables by global nodes to overcome these difficulties. The selection of these global nodes is important for the performance of the method and seems to be rather involved for linear elastostatics [13].

In [14, 20], we suggested the "all–floating" BETI method. Related numerical results were presented in [21]. In the meantime, the all-floating formulation was also applied for the coupling of FETI and BETI methods [15, 25]. This new version of the BETI method incooperates the Dirichlet boundary conditions by additional constraints in the dual formulation. This unifies the treatment of the subdomains, since all subdomains are considered as floating subdomains. Therefore, the implementation is simplified. Independently, the same idea has been introduced in [3] for FETI methods, called Total-FETI. Additionally, the all-floating version utilizes an improved condition number of the preconditioned local Steklov–Poincaré operators [19, 29] and shows a better asymptotic complexity.

In this paper, we present the all-floating BETI method for linear elasticity. The iterative inexact solution scheme, which we suggested in [14] for standard BETI methods, needs not more than $\mathcal{O}(1 + \log(H/h))$ iterations in the case of the all-floating formulation compared to $\mathcal{O}((1 + \log(H/h))^2)$ iterations for the standard BETI method. H denotes the diameter of a subdomain and h is the local meshsize. Therefore the all-floating formulation is asymptotically faster than the standard BETI formulation.

The paper is organized as follows: The primal Dirichlet domain decomposition method is described in Sect. 2 as a starting point of the later derivation of the BETI methods. In Sect. 3, we give a short introduction in the boundary element realization of the local Dirichlet to Neumann maps and present a suitable preconditioning strategy and the related spectral equivalence inequalities. The all-floating BETI method is described for linear elasticity in Sect. 4 in details. There, we state our main result on the computational complexity of the proposed method. Finally, two mixed boundary value problems of linear elastostatics are given as numerical examples in Sect. 5 indicating the improved complexity of the all-floating formulation.

2 Dirichlet Domain Decomposition Method

The mixed boundary value problem of linear elastostatics

$$\begin{aligned} -\operatorname{div}\sigma(\boldsymbol{u}, x) &= \mathbf{0} && \text{for } x \in \Omega \subset \mathbb{R}^3, \\ \gamma_0 \boldsymbol{u}(x) &= \boldsymbol{g}_D(x) && \text{for } x \in \Gamma_D, \\ \gamma_1 \boldsymbol{u}(x) &= \boldsymbol{g}_N(x) && \text{for } x \in \Gamma_N, \end{aligned} \tag{2.1}$$

is considered as model problem where $\Gamma = \partial\Omega = \overline{\Gamma}_D \cup \overline{\Gamma}_N$. For the sake of simplicity, we assume that Γ_D and Γ_N are identical for all three components. But all results apply, e.g.,

for the case of different decompositions for each component or for boundary conditions in normal and tangential directions, too. $\boldsymbol{u}(x)$ denotes the vectorial displacements. The relation of the stress tensor $\sigma(\boldsymbol{u})$ and the linearized strain tensor $e(\boldsymbol{u}) = \frac{1}{2}(\nabla \boldsymbol{u}^\top + \nabla \boldsymbol{u})$ is given by Hooke's law

$$\sigma(\boldsymbol{u}) = \frac{E\nu}{(1+\nu)(1-2\nu)} \text{tr } e(\boldsymbol{u}) I + \frac{E}{(1+\nu)} e(\boldsymbol{u}).$$

$E > 0$ denotes the elasticity module and $\nu \in (0, 1/2)$ is the Poisson ratio. The trace operators are defined by

$$\gamma_0 \boldsymbol{u}(x) := \lim_{\Omega \ni \widetilde{x} \to x \in \Gamma} \boldsymbol{u}(\widetilde{x}) \qquad \text{for almost all } x \in \Gamma$$

and

$$\gamma_1 \boldsymbol{u}(x) = \lambda \operatorname{div} \boldsymbol{u}(x) \boldsymbol{n}(x) + 2\mu \frac{\partial}{\partial n_x} \boldsymbol{u}(x) + \mu\, \boldsymbol{n}(x) \times \operatorname{curl} \boldsymbol{u}(x) \qquad \text{for almost all } x \in \Gamma,$$

where $\boldsymbol{n}$ is the exterior unit normal direction. Let the bounded Lipschitz domain Ω be decomposed into p non-overlapping subdomains Ω_i, i.e,

$$\overline{\Omega} = \bigcup_{i=1}^{p} \overline{\Omega}_i \quad \text{where } \Omega_i \cap \Omega_j = \emptyset \quad \text{for } i \neq j.$$

$\Gamma_i := \partial\Omega_i$ denotes the Lipschitz boundary of a subdomain. For neighboring subdomains the local coupling interface is given by $\Gamma_{ij} := \Gamma_i \cap \Gamma_j$ for all $i < j$. The skeleton of the domain decomposition is defined by

$$\Gamma_S := \bigcup_{i=1}^{p} \Gamma_i = \Gamma \cup \bigcup_{i<j} \overline{\Gamma}_{ij}.$$

The material parameters $E_i > 0$ and $\nu_i \in (0, 1/2)$ are assumed to be constant in each subdomain Ω_i. Thus, the global boundary value problem (2.1) can be rewritten by local boundary value problems

$$\begin{aligned} -\operatorname{div} \sigma(\boldsymbol{u}_i, x) &= 0 && \text{for } x \in \Omega_i, \\ \gamma_0^i \boldsymbol{u}_i(x) &= \boldsymbol{g}_D(x) && \text{for } x \in \Gamma_i \cap \Gamma_D, \\ \gamma_1^i \boldsymbol{u}_i(x) &= \boldsymbol{g}_N(x) && \text{for } x \in \Gamma_i \cap \Gamma_N \end{aligned} \tag{2.2}$$

and the transmission conditions

$$\gamma_0^i \boldsymbol{u}_i(x) = \gamma_0^j \boldsymbol{u}_j(x) \qquad \text{and} \qquad \gamma_1^i \boldsymbol{u}_i(x) + \gamma_1^j \boldsymbol{u}_j(x) = 0 \qquad \text{for } x \in \Gamma_{ij}.$$

γ_0^i and γ_1^i denote the trace operators of the subdomain Ω_i. Note that γ_1^i is defined with respect to the exterior normal direction of Ω_i. A basic tool is the local Dirichlet to Neumann

map including the so-called Steklov–Poincaré operator S_i which is defined by the traction $S_i \boldsymbol{f}_i(x) = \gamma_1^i \boldsymbol{v}_i(x)$ of the solution of the local Dirichlet boundary value problem

$$\begin{aligned} -\operatorname{div} \sigma(\boldsymbol{v}_i, x) &= 0 && \text{for } x \in \Omega_i, \\ \gamma_0^i \boldsymbol{v}_i(x) &= \boldsymbol{f}_i(x) && \text{for } x \in \Gamma_i. \end{aligned}$$

Next, local transmission problems can be formulated for $i = 1, \ldots, p$: *Find* $\boldsymbol{u}_i \in H^{1/2}(\Gamma_i)$ *such that*

$$\begin{aligned} \gamma_0^i \boldsymbol{u}_i(x) &= \boldsymbol{g}_D(x) && \text{for } x \in \Gamma_i \cap \Gamma_D, \\ \gamma_1^i \boldsymbol{u}_i(x) &= \boldsymbol{g}_N(x) && \text{for } x \in \Gamma_i \cap \Gamma_N, \\ \gamma_0^i \boldsymbol{u}_i(x) &= \gamma_0^j \boldsymbol{u}_j(x) && \text{for } x \in \Gamma_{ij}, \\ \gamma_1^i \boldsymbol{u}_i(x) + \gamma_1^j \boldsymbol{u}_j(x) &= \boldsymbol{0} && \text{for } x \in \Gamma_{ij} \\ \gamma_1^i \boldsymbol{u}_i(x) &= (S_i \boldsymbol{u}_i)(x) && \text{for } x \in \Gamma_i. \end{aligned}$$

Here, a Dirichlet domain decomposition method is considered first. The Neumann traces are replaced by the local Dirichlet to Neumann maps, $\gamma_1^i \boldsymbol{u}_i = S_i \boldsymbol{u}_i$, and a global function $\boldsymbol{u} \in \left[H^{1/2}(\Gamma_S)\right]^3$ is introduced to satisfy the continuity of the local functions $\boldsymbol{u}_i$ at the interfaces. In other words, the local functions $\boldsymbol{u}_i$ are the restrictions $\boldsymbol{u}_i = \boldsymbol{u}_{|\Gamma_i}$ of the global function $\boldsymbol{u}$ to the subdomain boundaries Γ_i. $H^{1/2}(\Gamma_S)$ is the trace space of $H^1(\Omega)$ on the skeleton Γ_S. The Dirichlet boundary conditions on Γ_D are considered as constraints of the function $\boldsymbol{u}$, whereas the Neumann transmission conditions and the Neumann boundary conditions are formulated in a variational sense by

$$\int_{\Gamma_{ij}} \left[(S_i \boldsymbol{u}_{|\Gamma_i})(x) + (S_j \boldsymbol{u}_{|\Gamma_j})(x)\right] \cdot \boldsymbol{v}_{ij}(x) ds_x = 0 \qquad \text{for all } \boldsymbol{v}_{ij} \in \left[H^{1/2}(\Gamma_{ij})\right]^3,\ i < j$$

and

$$\int_{\Gamma_i \cap \Gamma_N} \left[(S_i \boldsymbol{u}_{|\Gamma_i})(x) - \boldsymbol{g}_N(x)\right] \cdot \boldsymbol{v}_N(x) ds_x = 0 \qquad \text{for all } \boldsymbol{v}_N \in \left[H^{1/2}(\Gamma_N)\right]^3,\ i = 1, \ldots, p.$$

The sum over all coupling interfaces Γ_{ij} and the Neumann boundary Γ_N gives the variational formulation: *Find* $\boldsymbol{u} \in \left[H^{1/2}(\Gamma_S)\right]^3$ *with* $\boldsymbol{u} = \boldsymbol{g}_D$ *on* Γ_D *and*

$$\sum_{i=1}^{p} \int_{\Gamma_i} (S_i \boldsymbol{u}_{|\Gamma_i})(x) \cdot \widehat{\boldsymbol{v}}_{|\Gamma_i}(x) ds_x = \int_{\Gamma_N} \boldsymbol{g}_N(x) \cdot \widehat{\boldsymbol{v}}_{|\Gamma_N}(x) ds_x \qquad \text{for all } \widehat{\boldsymbol{v}} \in \left[H_0^{1/2}(\Gamma_S, \Gamma_D)\right]^3.$$

The test space $\left[H_0^{1/2}(\Gamma_S, \Gamma_D)\right]^3$ is defined by

$$\left[H_0^{1/2}(\Gamma_S, \Gamma_D)\right]^3 := \left\{\boldsymbol{v} \in \left[H^{1/2}(\Gamma_S)\right]^3 : \boldsymbol{v}(x) = \boldsymbol{0} \text{ for all } x \in \Gamma_D\right\}.$$

If the function $\boldsymbol{u} \in \left[H^{1/2}(\Gamma_S)\right]^3$ is split by $\boldsymbol{u} = \widehat{\boldsymbol{u}} + \widehat{\boldsymbol{g}}_D$, where $\widehat{\boldsymbol{g}}_D \in [H^1(\Omega)]^3$ is a suitable and bounded extension of the given boundary data $\boldsymbol{g}_D$ on Γ_S, the variational formulation

reads as: *Find* $\widehat{\boldsymbol{u}} \in \left[H_0^{1/2}(\Gamma_S, \Gamma_D)\right]^3$, *such that*

$$\sum_{i=1}^{p} \int_{\Gamma_i} (S_i \widehat{\boldsymbol{u}}_{|\Gamma_i})(x) \cdot \widehat{\boldsymbol{v}}_{|\Gamma_i}(x) ds_x = \int_{\Gamma_N} \boldsymbol{g}_N(x) \cdot \widehat{\boldsymbol{v}}_{|\Gamma_N}(x) ds_x - \sum_{i=1}^{p} \int_{\Gamma_i} (S_i \widehat{\boldsymbol{g}}_{D|\Gamma_i})(x) \cdot \widehat{\boldsymbol{v}}_{|\Gamma_i}(x) ds_x \tag{2.3}$$

holds for all $\widehat{\boldsymbol{v}} \in \left[H_0^{1/2}(\Gamma_S, \Gamma_D)\right]^3$.

The bilinear form defined by the left hand side is bounded and $\left[H_0^{1/2}(\Gamma_S, \Gamma_D)\right]^3$–elliptic, see e.g. [9, 27]. Thus, the Lemma of Lax–Milgram states the unique solvability of the variational problem (2.3).

A discretization using piecewise linear and continuous basis functions $\varphi_k \in S_h^1(\Gamma_S)$ on the skeleton gives the system of linear equations

$$S_h \underline{\widehat{u}} = \sum_{i=1}^{p} A_i^\top S_{i,h} A_i \underline{\widehat{u}} = \sum_{i=1}^{p} A_i^\top \underline{f}_i + \sum_{i=1}^{p} A_i^\top \underline{f}_{N,i}, \tag{2.4}$$

where we use a blockwise notation separating the components of the physical quantities, in particular,

$$\underline{\widehat{u}} = \begin{pmatrix} \underline{\widehat{u}}^1 \\ \underline{\widehat{u}}^2 \\ \underline{\widehat{u}}^3 \end{pmatrix}, \quad S_{i,h} = \begin{pmatrix} S_{i,h}^{11} & S_{i,h}^{12} & S_{i,h}^{13} \\ S_{i,h}^{21} & S_{i,h}^{22} & S_{i,h}^{23} \\ S_{i,h}^{31} & S_{i,h}^{32} & S_{i,h}^{33} \end{pmatrix} \quad \boldsymbol{\varphi}_\ell^n := \begin{pmatrix} \delta_{1n} \\ \delta_{2n} \\ \delta_{3n} \end{pmatrix} \varphi_\ell$$

using the Kronecker symbol δ_{ij}. The blocks $S_{i,h}^{mn}$ of the matrix $S_{i,h}$ of the local Steklov–Poincairé operators are given by

$$S_{i,h}^{mn}[k, \ell] = \langle S_i \boldsymbol{\varphi}_\ell^n, \boldsymbol{\varphi}_k^m \rangle_{\Gamma_i}.$$

The connectivity matrices $A_i \in \mathbb{R}^{3\widehat{M}_i \times 3\widehat{M}}$ map the global nodes to the local ones and the global vector $\underline{v}$ to the local ones $\underline{v}_i = A_i \underline{v}$ componentwise. $\widehat{M}_i = M_{C,i} + M_{N,i}$ is the number of all non-Dirichlet nodes, i.e., coupling and Neumann nodes, on Γ_i, and $\widehat{M}$ is their number on the whole skeleton Γ_S. The coefficients of the block vector $\underline{f}_{N,i}^m$ of the vectors $\underline{f}_{N,i}$ are given by

$$f_{N,i}^m[k] = \begin{cases} \displaystyle\int_{\Gamma_N \cap \Gamma_i} \boldsymbol{g}_N(x) \cdot \boldsymbol{\varphi}_{k|\Gamma_N}^m(x) ds_x & \text{if supp } \varphi_k \cap (\Gamma_N \cap \Gamma_i) \neq \emptyset \\ 0 & \text{else,} \end{cases}$$

and those of the vectors $\underline{f_i}$ by

$$f_i^m[k] = -\int_{\Gamma_i} (S_i \widehat{\boldsymbol{g}}_{D|\Gamma_i})(x) \cdot \boldsymbol{\varphi}_{k|\Gamma_i}^M(x) ds_x.$$

Note that the system (2.4) of linear equations is uniquely solvable, and if we assume $\boldsymbol{u} \in [H^2(\Gamma_S)]^3$, we will get an optimal order of convergence of 1.5 for lowest order elements with respect to the meshsize h, see, e.g., [16, 27].

3 Boundary Element Approximation and Preconditioning of the Local Operators

In this section, we will describe the boundary element approximation of the local Steklov–Poincaré operators first. For details on boundary integral equations and boundary element methods see, e.g., [10, 18] and [26, 28]. Further, we will discuss the invertibility of the Steklov–Poincaré operators and present an appropriate preconditioner using the concept of operators of opposite order [29].

3.1 Boundary Element Realization of the Local Steklov–Poincaré Operator

The solution of boundary value problems like (2.2) can be given by the representation formula

$$\boldsymbol{u}_i(x) = \int_\Gamma \gamma^i_{0,y} U^*(x,y) \gamma^i_1 \boldsymbol{u}_i(y) ds_y - \int_\Gamma \left(\gamma^i_{1,y} U^*(x,y)\right)^\top \gamma^i_0 \boldsymbol{u}_i(y) ds_y$$

for $x \in \Omega_i$. The fundamental solution of linear elasticity is given by Kelvin's tensor

$$U^*_{k\ell}(x,y) = \frac{1}{8\pi}\frac{1}{E}\frac{1+\nu}{1-\nu}\left[(3-4\nu)\frac{\delta_{k\ell}}{|x-y|} + \frac{(x_k-y_k)(x_\ell-y_\ell)}{|x-y|^3}\right] \qquad \text{for } k,\ell = 1,\ldots,3.$$

Thus the knowledge of the complete Cauchy data $\gamma^i_0 \boldsymbol{u}_i$ and $\gamma^i_1 \boldsymbol{u}_i$ on the subdomain boundary Γ_i is sufficient to compute the solution. In domain decomposition the knowledge of the Cauchy data is even sufficient for solving the coupled problem. The unknown Cauchy data can be determined from the first boundary integral equation

$$\gamma^i_0 \boldsymbol{u}_i = (\frac{1}{2} I - K_i)\gamma^i_0 \boldsymbol{u}_i + V_i \gamma^i_1 \boldsymbol{u}_i \tag{3.5}$$

and the second hypersingular boundary integral equation

$$\gamma^i_1 \boldsymbol{u}_i = D_i \gamma^i_0 \boldsymbol{u}_i + (\frac{1}{2} I + K'_i)\gamma^i_1 \boldsymbol{u}_i. \tag{3.6}$$

V_i denotes the single layer potential

$$(V_i \boldsymbol{t}_i)(x) = \int_{\Gamma_i} U^*(x,y)\boldsymbol{t}_i(y) ds_y \qquad \text{for } x \in \Gamma_i,$$

K_i the double layer potential

$$(K_i \boldsymbol{u}_i)(x) = \int_{\Gamma_i \setminus \{x\}} T^*(x,y)\boldsymbol{u}_i ds_y \qquad \text{for } x \in \Gamma_i,$$

where $T^*(x,y) = (\gamma^i_{1,y} U^*(x,y))^\top$, K'_i the adjoint double layer potential

$$(K'_i \boldsymbol{t}_i)(x) = \int_{\Gamma_i \setminus \{x\}} \gamma^i_{1,x} U^*(x,y)\boldsymbol{t}_i(y) ds_y \qquad \text{for } x \in \Gamma_i,$$

and D_i the hypersingular operator

$$(D_i \boldsymbol{u}_i)(x) = -\gamma_{1,x}^i \int_{\Gamma_i} T^*(x,y)\boldsymbol{u}_i(y) ds_y \qquad \text{for } x \in \Gamma_i.$$

Due to the ellipticity and invertibility of the single layer potential V_i, the boundary integral equation (3.5) can be written as

$$\gamma_1^i \boldsymbol{u}_i = V_i^{-1}(\frac{1}{2}I + K_i)\gamma_0^i \boldsymbol{u}_i \tag{3.7}$$

This already defines a Dirichlet to Neumann map but its boundary element discretization realizes a non-symmetric approximation of the self-adjoint operator S_i. But plugging (3.7) into the hypersingular boundary integral equation (3.6) results in a second representation of the Dirichlet to Neumann map

$$\gamma_1^i \boldsymbol{u}_i = S_i \gamma_0^i \boldsymbol{u}_i = \left(D_i + (\frac{1}{2}I + K_i')V_i^{-1}(\frac{1}{2}I + K_i) \right) \gamma_0^i \boldsymbol{u}_i,$$

which will lead to a symmetric Galerkin boundary element approximation. Here, we use a regular quasi-uniform boundary element mesh with meshsize h for the discretization. The displacement $\gamma_0^i \boldsymbol{u}_i$ is approximated componentwise by the space $S_h^1(\Gamma_i) = \text{span } \{\varphi_k\}_{k=1}^{M_i}$ of piecewise linear and globally continuous basis functions φ_k and the traction $\gamma_1^i \boldsymbol{u}_i$ is approximated componentwise by the space $S_h^0(\Gamma_i) = \text{span } \{\psi_\ell\}_{\ell=1}^{N_i}$ of piecewise constant basis functions ψ_ℓ. M_i and N_i denote the number of nodes and the number of triangles of the mesh of Ω_i, respectively.

As the inverse operator V_i^{-1} of the single layer potential is not available in general, we define an approximation $\widetilde{S}_i$ of the Steklov–Poincaré operator S_i by

$$\widetilde{S}_i \boldsymbol{u}_i = D_i \boldsymbol{u}_i + (\frac{1}{2}I + K_i')\boldsymbol{t}_{i,h},$$

where $\boldsymbol{t}_{i,h} \in [S_h^0(\Gamma_i)]^3$ is defined by an approximation of the inverse single layer potential by

$$\langle V \boldsymbol{t}_{i,h}, \boldsymbol{\tau}_{i,h} \rangle_{\Gamma_i} = \langle (\frac{1}{2}I + K)\boldsymbol{u}_i, \boldsymbol{\tau}_{i,h} \rangle_{\Gamma_i} \qquad \text{for all } \boldsymbol{\tau}_{i,h} \in \left[S_h^0(\Gamma_i)\right]^3,$$

with the duality pairing

$$\langle \boldsymbol{w}, \boldsymbol{v} \rangle_{\Gamma_i} = \int_{\Gamma_i} \boldsymbol{w}(x) \cdot \boldsymbol{v}(x) ds_x.$$

Note that there holds an error estimate for this approximation

$$\|(S_i - \widetilde{S}_i)\boldsymbol{u}_i\|_{\left[H^{-1/2}(\Gamma_i)\right]^3} \leq c \inf_{\boldsymbol{\tau}_{i,h} \in \left[S_h^0(\Gamma_i)\right]^3} \|S_i \boldsymbol{u}_i - \boldsymbol{\tau}_{i,h}\|_{\left[H^{-1/2}(\Gamma_i)\right]^3}, \tag{3.8}$$

see, e.g., [27]. This estimate is sufficient to recover the asymptotically optimal error estimates for the solution of the local boundary value problems and the coupled problem.

Finally, we are able to define a boundary element approximation $\widetilde{S}_{i,h}$ of the discrete Steklov–Poincaré operator $S_{i,h}$ used in (2.4) by

$$\widetilde{S}_{i,h} = D_{i,h} + (\frac{1}{2}M_{i,h}^\top + K_{i,h}^\top)V_{i,h}^{-1}(\frac{1}{2}M_{i,h} + K_{i,h}),$$

where the blocks of the involved matrices are given by

$$\begin{aligned} V_{i,h}^{mn}[\ell,k] &= \langle V_i\boldsymbol{\psi}_k^n, \boldsymbol{\psi}_\ell^m\rangle_{\Gamma_i}, & K_{i,h}^{mn}[\ell,i] &= \langle K_i\boldsymbol{\varphi}_i^n, \boldsymbol{\psi}_\ell^m\rangle_{\Gamma_i}, \\ M_{i,h}^{mn}[j,k] &= \langle \boldsymbol{\varphi}_i^n, \boldsymbol{\psi}_\ell^m\rangle_{\Gamma_i}, & D_{i,h}^{mn}[j,i] &= \langle D_i\boldsymbol{\varphi}_i^n, \boldsymbol{\varphi}_j^m\rangle_{\Gamma_i} \end{aligned}$$

for $k,\ell = 1,\ldots,N_i$ and $i,j = 1,\ldots,M_i$.

3.2 Inversion and Preconditioning of the Local Steklov–Poincaré Operator

For the formulation of the BETI method, we will need the inverse of the local Steklov–Poincaré operator S_i. The application $\gamma_0^i\boldsymbol{u}_i = S_i^{-1}\boldsymbol{g}$ of the inverse of S_i corresponds to the solution of the Neumann boundary value problem

$$\begin{aligned} -\operatorname{div}\sigma(\boldsymbol{u}_i,x) &= \boldsymbol{0} && \text{for } x\in\Omega_i\subset\mathbb{R}^3, \\ \gamma_1^i\boldsymbol{u}_i(x) &= \boldsymbol{g}(x) && \text{for } x\in\Gamma_i. \end{aligned}$$

The solution of such a Neumann boundary value problem is only unique up to the rigid body motions

$$\boldsymbol{v}_{1,i} = \begin{pmatrix}1\\0\\0\end{pmatrix}, \boldsymbol{v}_{2,i} = \begin{pmatrix}0\\1\\0\end{pmatrix}, \boldsymbol{v}_{3,i} = \begin{pmatrix}0\\0\\1\end{pmatrix}, \boldsymbol{v}_{4,i} = \begin{pmatrix}-x_2\\x_1\\0\end{pmatrix}, \boldsymbol{v}_{5,i} = \begin{pmatrix}0\\-x_3\\x_2\end{pmatrix}, \boldsymbol{v}_{6,i} = \begin{pmatrix}x_3\\0\\-x_1\end{pmatrix},$$

which are the solutions of the homogeneous Neumann boundary value problem. From Betti's second formula we get the solvability conditions

$$\int_{\Gamma_i}\gamma_0^i\boldsymbol{v}_{k,i}(x)\cdot\boldsymbol{g}(x)ds_x = 0 \qquad \text{for } k = 1,\ldots,6. \tag{3.9}$$

The rigid body motions form the kernel of the hypersingular operator D_i and the kernel of $(1/2I + K_i)$, too. Eliminating the rigid body motions from the Sobolev space $\left[H^{1/2}(\Gamma_i)\right]^3$ admits a unique solution of the Neumann boundary value problem, see, e.g., [23, 28].

Since we have to define an orthogonality relation in $\left[H^{1/2}(\Gamma_i)\right]^3$, we use the scalar product induced by the componentwise application of the inverse of the single layer potential $V_{L,i}$ of the Laplacian to define an orthogonal complement of the kernel of the Steklov–Poincaré operator S_i. This admits the definition of a stabilized Steklov–Poincaré operator $\widehat{S}_i$ [20] by

$$\begin{aligned} \langle\widehat{S}_i\boldsymbol{u}_i,\boldsymbol{v}_i\rangle_{\Gamma_i} \;:=\; & \langle D_i\boldsymbol{u}_i,\boldsymbol{v}_i\rangle_{\Gamma_i} + \sum_{k=1}^{6}\alpha_{k,i}\langle\boldsymbol{u}_i,\widetilde{\boldsymbol{w}}_{k,i}\rangle_{\Gamma_i}\langle\boldsymbol{v}_i,\widetilde{\boldsymbol{w}}_{k,i}\rangle_{\Gamma_i} \\ & + \langle(\frac{1}{2}I + K_i')V_i^{-1}(\frac{1}{2}I + K_i)\boldsymbol{u}_i,\boldsymbol{v}_i\rangle_{\Gamma_i}. \end{aligned} \tag{3.10}$$

The functions $\widetilde{\boldsymbol{w}}_{k,i}$ form an orthogonal basis of the set of functions spanned by $\widetilde{\boldsymbol{v}}_{k,i} = \widehat{V}_i^{-1}\boldsymbol{v}_{k,i}, k = 1,\dots,6$ where $\widehat{V}_i^{mn} = \delta_{nm}V_{L,i}$ These functions can be computed by the method of Gram–Schmidt with four applications of $V_{L,i}^{-1}$. On the discrete level, the required computational costs are much smaller than solving a boundary value problem of linear elasticity. The stabilized Steklov–Poincaré operator $\widehat{S}_i$ is $\left[H^{1/2}(\Gamma_i)\right]^3$–elliptic [20]. Thus, $\widehat{S}_i$ is invertible and defines a pseudoinverse which we will need for the formulation of the BETI methods.

We use the technique of operators of opposite order [29] to define a preconditioner for the iterative inversion of $\widehat{S}_i$. We present spectral equivalence inequalities for $\widehat{S}_i$ and $\widehat{V}_i^{-1}$. The specific construction of the modified Steklov–Poincaré operator $\widehat{S}_i$ is essential for this estimate. For optimal inequality constants, we choose the parameters

$$\alpha_{k,i} = \frac{1}{4}\frac{E_i}{1-2\nu_i}\frac{1-\nu_i}{1+\nu_i}\frac{1}{\langle\widetilde{\boldsymbol{v}}_{k,i},\widetilde{\boldsymbol{w}}_{k,i}\rangle_{\Gamma_i}}. \tag{3.11}$$

Theorem 1 ([20])**.** *For the single layer potential $V_{L,i}$ of the Laplacian and for the modified Steklov–Poincaré operator $\widehat{S}_i$ there hold the spectral equivalence inequalities*

$$c_1^{V_L}\widetilde{c}_1^{D}\langle\widehat{V}_i^{-1}\boldsymbol{u}_i,\boldsymbol{u}_i\rangle_{\Gamma_i} \le \langle\widehat{S}\boldsymbol{u}_i,\boldsymbol{u}_i\rangle_{\Gamma_i} \le (1/4+c_K)\frac{E_i}{1-2\nu_i}\frac{1-\nu_i}{1+\nu_i}\langle\widehat{V}_i^{-1}\boldsymbol{u}_i,\boldsymbol{u}_i\rangle_{\Gamma_i} \tag{3.12}$$

for all $\boldsymbol{u}_i \in \left[H^{1/2}(\Gamma_i)\right]^3$ with the ellipticity constant $c_1^{V_L}$ of the single layer potential $V_{L,i}$ of the Laplacian and the ellipticity constant $\widetilde{c}_1^{D}$ of the modified hypersingular operator in the orthogonal space of its kernel with respect to the scalar product induced by $\widehat{V}_i^{-1}$. Further,

$$c_K = \frac{1}{2} + \sqrt{\frac{1}{2} - c_1^V c_1^D} < 1$$

is the contraction constant of the double layer potential K_i,

$$\|(\frac{1}{2}I + K_i)\boldsymbol{u}_i\|_{V_i^{-1}} \le c_K\|\boldsymbol{u}_i\|_{V_i^{-1}} \qquad \textit{for all } \boldsymbol{u}_i \in \left[H^{1/2}(\Gamma_i)\right]^3.$$

Note that the constants of the estimates are independent of the discretization, but depend on the shape of the domain Ω_i.

As preconditioner of the discrete approximation $\widehat{S}_{i,h}$ of the stabilized Steklov–Poincaré operator $\widehat{S}_i$,

$$\widehat{S}_{i,h} = \widetilde{S}_{i,h} + \sum_{k=1}^{6}\alpha_{k,i}\underline{a}_{k,i}\underline{a}_{k,i}^{\top} \qquad \text{where } a_{k,i}^n[j] = \langle\boldsymbol{\varphi}_j^n,\widetilde{\boldsymbol{w}}_k\rangle_{\Gamma_i}, \tag{3.13}$$

we can use the approximation

$$\widetilde{C}_{D,i} := \widetilde{M}_{i,h}\widehat{V}_{i,h}^{-1}\widetilde{M}_{i,h} \tag{3.14}$$

with the entries of the matrix blocks

$$\widehat{V}_{i,h}^{mn}[j,\ell] = \delta_{nm}\langle V_{L,i}\varphi_\ell,\varphi_j\rangle_{\Gamma_i} \qquad \text{and} \qquad \widetilde{M}_{i,h}^{mn}[j,\ell] = \delta_{nm}\langle\varphi_\ell,\varphi_j\rangle_{\Gamma_i}$$

for $j, \ell = 1, \ldots, M_i$, which is spectrally equivalent to $S_{i,h}$ [28, 29]. As we apply the inverse of $\widetilde{C}_D$ in the iterative solver, we need the application of $\widehat{V}_{i,h}$ and the inexpensive inversion of the mass matrix $\widetilde{M}_{i,h}$ only.

Remark 1. *In the case that S_i is defined on an open subset $\Gamma_{i,0}$ of Γ_i, the estimates worsen by a polylogarithmic factor [19]. Thus, the iteration numbers grow logarithmically compared to the case of the closed boundary Γ_i, where the iteration numbers for solving the preconditioned system are bounded, since the estimates (3.12) are independent of the meshsize h.*

4 The All-Floating BETI Formulation

We consider the system (2.4) of linear equations for the primal Dirichlet domain decomposition method and the corresponding minimization problem

$$\widehat{\underline{u}} = \arg\min_{\widehat{\underline{w}} \in \mathbb{R}^{3\widehat{M}}} \sum_{i=1}^{p} \left[\frac{1}{2} (\widetilde{S}_{i,h} A_i \widehat{\underline{w}}, A_i \widehat{\underline{w}}) - (\underline{f}_i, A_i \widehat{\underline{w}}) - (\underline{f}_{N,i}, A_i \widehat{\underline{w}}) \right],$$

respectively. The main ideas of the Tearing and Interconnecting method [6, 7] are the tearing of the global degrees of freedom $\widehat{\underline{u}}$ in local degrees of freedom $\widehat{\underline{u}}_i = A_i \widehat{\underline{u}}$ and the interconnecting of the local degrees of freedom $\widehat{\underline{u}}_i$ at the coupling interfaces Γ_{ij} by constraints. The resulting Schur complement system of the standard BETI method [16] reads as

$$\sum_{i=1}^{q} B_i \widehat{S}_{i,h}^{-1} B_i^\top \underline{\lambda} + \sum_{i=q+1}^{p} B_i \widetilde{S}_{i,h}^{-1} B_i^\top \underline{\lambda} + G\underline{\gamma} = -\sum_{i=1}^{q} B_i \widehat{S}_{i,h}^{-1} (\underline{f}_i + \underline{f}_{N,i}) - \sum_{i=q+1}^{p} B_i \widetilde{S}_{i,h}^{-1} (\underline{f}_i + \underline{f}_{N,i}) \tag{4.15}$$

where $G = (B_1 \underline{v}_{1,1}, \ldots, B_1 \underline{v}_{\dim \mathcal{R}_1,1}, \ldots, B_q \underline{v}_{\dim \mathcal{R}_q,q}) \in \mathbb{R}^{3M_L \times q \dim \mathcal{R}}$, see, e.g. [16, 20]. We will present a detailed derivation for the all-floating version later. Here, one has to distinguish whether the local subproblem is uniquely solvable due to sufficient Dirichlet boundary conditions or not. We assume that the first q local subproblems are not uniquely solvable ($i = 1, \ldots, q$) and a pseudoinverse $\widehat{S}_i^{-1}$, which can be defined as presented in Sect. 3.2, has to be used. These subdomains are called floating subdomains. The Steklov–Poincaré operators of the remaining subdomains ($i = q+1, \ldots, p$) are invertible. M_L is the total number of constraints per component and $\dim \mathcal{R}_i$ denotes the number of active rigid body motions of subdomain Ω_i.

A projection method [2, 11] is used to solve the BETI Schur complement system (4.15), see also Sect. 4.1. For the stabilized Steklov–Poincaré operator $\widehat{S}_{i,h}$, the active rigid body motions of the subdomain Ω_i have to be determined. While this can be decided easily in the case of the Laplacian, this task is not trivial in the case of linear elastostatics, depending on given boundary and transmission conditions. An approach avoiding these difficulties is the dual primal formulation of the Tearing and Interconnection methods, called FETI–DP

[4, 5, 13]. This method reintroduces a set of global nodes and the corresponding primal variables to make the local Steklov–Poincaré operators invertible, while the continuity is guaranteed for the remaining coupling nodes by the constraints. The choice of the primal variables is important for the robustness and the efficiency of the method and seems to be rather involved in the case of linear elastostatics [13].

Here, we will present the all-floating formulation of the BETI method which unifies the treatment of the subdomains as all are considered as floating. This simplifies the implementation and a change of the boundary conditions, as for example in contact problems, does not effect the method. The condition number of the local Steklov–Poincaré operator preconditioned by the operator of opposite order increases logarithmically for a non-floating subdomain while it is bounded for a floating subdomain, see Sect. 3.2. The all-floating formulation benefits from this fact with an improved asymptotic complexity.

The all-floating formulation of the BETI method is derived starting from the system (2.4) of linear equations

$$\widetilde{S}_h \widehat{\underline{u}} = \sum_{i=1}^{p} A_i^\top \widetilde{S}_{i,h} A_i \widehat{\underline{u}} = \sum_{i=1}^{p} A_i^\top \underline{f}_i + \sum_{i=1}^{p} A_i^\top \underline{f}_{N,i}$$

and the corresponding minimization problem

$$\widehat{\underline{u}} = \arg\min_{\widehat{\underline{w}} \in \mathbb{R}^{3\widehat{M}}} \sum_{i=1}^{p} \left[\frac{1}{2} (\widetilde{S}_{i,h} A_i \widehat{\underline{w}}, A_i \widehat{\underline{w}}) - (\underline{f}_i, A_i \widehat{\underline{w}}) - (\underline{f}_{N,i}, A_i \widehat{\underline{w}}) \right],$$

respectively. Note that the vectors $\widehat{\underline{w}}$ have no entries related to nodes of the Dirichlet boundary Γ_D, as the corresponding functions $\widehat{\boldsymbol{w}}_h$ vanish on this part of the boundary. As in the standard BETI method, local vectors $\widehat{\underline{w}}_i = A_i \widehat{\underline{w}}$ are introduced and constraints are set up to guarantee the continuity across the interfaces. Thus, local minimization problems

$$\widehat{\underline{u}}_i = \arg\min_{\widehat{\underline{w}}_i \in \mathbb{R}^{3\widehat{M}_i}} \frac{1}{2} (\widetilde{S}_{i,h} \widehat{\underline{w}}_i, \widehat{\underline{w}}_i) - (\underline{f}_i, \widehat{\underline{w}}_i) - (\underline{f}_{N,i}, \widehat{\underline{w}}_i) \tag{4.16}$$

have to be solved. These are interconnected by the constraints

$$\sum_{i=1}^{p} B_i \widehat{\underline{u}}_i = \underline{0}.$$

$n-1$ non-redundant constraints are assigned to a global coupling node adjacent to n subdomains. The total number of constraints is denoted by $3M_L$. The constraints are applied to up to three components at the nodes in linear elastostatics. The components of the local vectors $\widehat{\underline{u}}_i$ are connected to the subdomain Ω_j with the largest coefficient $E_j/(1+\nu_j)$, see [11]. For each subdomain Ω_k with $k \neq j$ which includes the coupling node, a constraint is stated with a global index r. The corresponding entries of the blocks B_i^{mn} of the matrices B_i are

$$B_i^{mn}[r,s] = \delta_{nm} \begin{cases} 1 & \text{for } i = j \text{ and } s = \ell_j, \\ -1 & \text{for } i = k \text{ and } s = \ell_k, \\ 0 & \text{else,} \end{cases} \tag{4.17}$$

where ℓ_j is the local index of the coupling node in the subdomain Ω_j corresponding to the related block of the connectivity matrices A_j. For a redundant version of the constraints, see e.g. [11, 30].

Until here, the all-floating approach is identical to the standard Tearing and Interconnecting methods. Next, the local vectors $\widehat{\underline{w}}_i$ and the related functions are extended to the whole boundary Γ_i of the subdomains. The symmetry of the Steklov–Poincaré operators is used for the splitting

$$(\underline{f}_i, \widehat{\underline{w}}_i) = -(\widetilde{S}_{i,h}\widehat{\underline{g}}_i, \widehat{\underline{w}}_i) = -\frac{1}{2}(\widetilde{S}_{i,h}\widehat{\underline{g}}_i, \widehat{\underline{w}}_i) - \frac{1}{2}(\widehat{\underline{g}}_i, \widetilde{S}_{i,h}\widehat{\underline{w}}_i).$$

where $\widehat{\underline{g}}_i$ is the vector corresponding to the linear interpolation of the extension $\widehat{\boldsymbol{g}}_D$ on Γ_i. The local vector $\widehat{\underline{w}}_i$ and the interpolation $\widehat{\underline{g}}_i$ of the Dirichlet datum are reunited to extend the related function to the whole boundary. The local minimization problems (4.16) are transformed to

$$\begin{aligned}
\widehat{\underline{u}}_i &= \underset{\widehat{\underline{w}}_i \in \mathbb{R}^{3\widehat{M}_i}}{\arg\min} \left\{ \frac{1}{2}(\widetilde{S}_{i,h}\widehat{\underline{w}}_i, \widehat{\underline{w}}_i) + \frac{1}{2}(S_{i,h}\widehat{\underline{g}}_i, \widehat{\underline{w}}_i) + \frac{1}{2}(\widehat{\underline{g}}_i, S_{i,h}\widehat{\underline{w}}_i) - (\underline{f}_{N,i}, \widehat{\underline{w}}_i) \right\} \\
&= \underset{\widehat{\underline{w}}_i \in \mathbb{R}^{3\widehat{M}_i}}{\arg\min} \left\{ \frac{1}{2}(\widetilde{S}_{i,h}(\widehat{\underline{w}}_i + \widehat{\underline{g}}_i), \widehat{\underline{w}}_i + \widehat{\underline{g}}_i) - (\underline{f}_{N,i}, \widehat{\underline{w}}_i + \widehat{\underline{g}}_i) - \frac{1}{2}(S_{i,h}\widehat{\underline{g}}_i, \widehat{\underline{g}}_i) + (\underline{f}_{N,i}, \widehat{\underline{g}}_i) \right\}.
\end{aligned}$$

As the solutions of the minimization problems do not depend on the constants of the last two terms, we consider the equivalent local minimization problems

$$\widehat{\underline{u}}_i = \underset{\widehat{\underline{w}}_i \in \mathbb{R}^{3\widehat{M}_i}}{\arg\min} \left\{ \frac{1}{2}(\widetilde{S}_{i,h}(\widehat{\underline{w}}_i + \widehat{\underline{g}}_i), \widehat{\underline{w}}_i + \widehat{\underline{g}}_i) - (\underline{f}_{N,i}, \widehat{\underline{w}}_i + \widehat{\underline{g}}_i) \right\}.$$

Defining new local functions $\boldsymbol{w}_{i,h} = \widehat{\boldsymbol{w}}_{i,h} + \widehat{\boldsymbol{g}}_{i,h}$ and their related vectors $\underline{w}_i \in \mathbb{R}^{3M_i}$, where M_i is the number of all nodes of the subdomain Ω_i, we get the minimization problems

$$\underline{u}_i = \underset{\underline{w}_i \in \mathbb{R}^{3M_i}}{\arg\min} \left\{ \frac{1}{2}(\widetilde{S}_{i,h}\underline{w}_i, \underline{w}_i) - (\underline{f}_{N,i}, \underline{w}_i) \right\}.$$

Extra constraints are used to satisfy the Dirichlet boundary conditions. Therefore, the system of constraints is extended to

$$\sum_{i=1}^{p} \widetilde{B}_i \underline{u}_i = \underline{b}$$

where $\widetilde{B}_i \in \mathbb{R}^{3(M_L + \sum_i M_{D,i}) \times 3M_i}$. In the case of a suitable ordering of the nodes, the entries of the matrix blocks are given by

$$\widetilde{B}_i^{nm}[j,k] = \delta_{nm} \begin{cases} B_i[j,k] & \text{if } j \leq M_L \\ 1 & \text{if } j > M_L \text{ and } k \text{ is the local index of a Dirichlet node } j \\ & \text{of the subdomain } \Omega_i, \\ 0 & \text{else.} \end{cases}$$

The entries of the right hand side $\underline{b}$ are given by

$$b^m[j] = \begin{cases} 0 & \text{if } j \leq M_L, \text{i.e. row } j \text{ is related to the coupling,} \\ g_D^m(x_k) & \text{if } j > M_L \text{ and } k \text{ is the local index of a Dirichlet node } j \\ & \text{of the subdomain } \Omega_i, \\ 0 & \text{else.} \end{cases}$$

Introducing Lagrangian multipliers $\underline{\lambda} \in \mathbb{R}^{3\widetilde{M}_L}$ results in the system of linear equations

$$\begin{pmatrix} \widetilde{S}_{1,h} & & & -\widetilde{B}_1^\top \\ & \ddots & & \vdots \\ & & \widetilde{S}_{p,h} & -\widetilde{B}_p^\top \\ \widetilde{B}_1 & \dots & \widetilde{B}_p & 0 \end{pmatrix} \begin{pmatrix} \underline{u}_1 \\ \vdots \\ \underline{u}_p \\ \underline{\lambda} \end{pmatrix} = \begin{pmatrix} \underline{f}_{N,1} \\ \vdots \\ \underline{f}_{N,p} \\ \underline{b} \end{pmatrix}, \tag{4.18}$$

where $\widetilde{M}_L = M_L + \sum_{i=1}^p M_{D,i}$ is the total number of Lagrangian multipliers of the all-floating version per component.

The main difference of this formulation to the standard BETI formulation is that the local functions and operators are now defined with respect to the whole boundary of the subdomains and that the number of constraints is increased. Thus, the total number of degrees of freedom and the memory requirements are increased. On the other hand, the preconditioning of the local operators is now independent of the discretization and all subdomains can be treated uniformly. The additional constraints of the Dirichlet boundary conditions are local and are not part of the communication of the parallel solver.

4.1 Projection Method and Preconditioning

The local Steklov–Poincaré operators and their discrete realizations $\widetilde{S}_{i,h}$ are not invertible anymore since they are now defined on the whole boundary Γ_i. Therefore, the stabilized pseudo inverse (3.13) is used. For any subdomain the local equations of (4.18)

$$\widetilde{S}_{i,h}\underline{u}_i = \underline{f}_{N,i} + \widetilde{B}_i^\top \underline{\lambda} \tag{4.19}$$

are solvable if the compatibility conditions, see (3.9),

$$(\underline{f}_{N,i} + \widetilde{B}_i^\top \underline{\lambda}, \underline{v}_{k,i}) = 0 \qquad \text{for all } k = 1, \dots, 6 \tag{4.20}$$

are satisfied for the rigid body motions $\underline{v}_{k,i} \in \mathbb{R}^{3M_i}$. Due to Sect. 3.2, the modified problems

$$\widehat{S}_{i,h}\underline{u}_i = \left[\widetilde{S}_{i,h} + \sum_{k=1}^{6} \alpha_{k,i} \underline{a}_{k,i}\, \underline{a}_{k,i}^\top \right] \underline{u}_i = \underline{f}_{N,i} + \widetilde{B}_i^\top \underline{\lambda}$$

are solved on the normalization condition

$$(\underline{a}_{k,i}, \underline{u}_i) = 0 \qquad \text{for } k = 1, \dots, 6.$$

$\alpha_{k,i}$ are the scaling parameters given in (3.11). Thus the solutions of the local problems (4.19) are given by

$$\underline{u}_i = \widehat{S}_{i,h}^{-1}(\underline{f}_{N,i} + \widetilde{B}_i^\top \underline{\lambda}) + \sum_{k=1}^{6} \gamma_{k,i}\underline{v}_{k,i} \qquad \text{for } i = 1, \ldots, p. \tag{4.21}$$

The constants $\gamma_{k,i} \in \mathbb{R}$ have to be determined from the global problem. Using the local solutions in the system (4.18) of linear equations results in the all-floating BETI Schur complement system

$$\sum_{i=1}^{p} \widetilde{B}_i \widehat{S}_{i,h}^{-1} \widetilde{B}_i^\top \underline{\lambda} + G\underline{\gamma} = \underline{b} - \sum_{i=1}^{p} \widetilde{B}_i \widehat{S}_{i,h}^{-1} \underline{f}_{N,i}, \tag{4.22}$$

where $G = (\widetilde{B}_1\underline{v}_{1,1}, \ldots, \widetilde{B}_1\underline{v}_{6,1}, \ldots, \widetilde{B}_p\underline{v}_{6,p}) \in \mathbb{R}^{3\widetilde{M}_L \times 6p}$. This defines the system of linear equations

$$F\underline{\lambda} + G\underline{\gamma} = \underline{d}. \tag{4.23}$$

The compatibility conditions (4.20) can be rewritten as

$$G^\top \underline{\lambda} = -\left((\underline{f}_{N,i}, \underline{v}_{k,i})\right)_{k=1:6, i=1:q} =: \underline{e}. \tag{4.24}$$

In the Tearing and Interconnecting methods, a projection $P = I - QG(G^\top QG)^{-1}G^\top$ of the image $\mathrm{Im}\,(\widetilde{B})$ to the subspace $\mathrm{Ker}\,(G^\top) = (\mathrm{Im}\,(G))^\perp$ is used with a suitable diagonal scaling matrix Q [2, 11]. If all constraints of a global coupling node are built with respect to the subdomain with the largest coefficient, the entries of the diagonal matrix are chosen as, see [11, 12]

$$Q^{nm}[\ell,\ell] = \delta_{nm} \begin{cases} \mu_i \left(1 + \log\left(\dfrac{H_i}{h_i}\right)\right) \dfrac{h_i^2}{H_i} & \text{if the node } x_\ell \text{ is inside a subdomain face,} \\ \mu_i\, h_i & \text{if the node } x_\ell \text{ is inside a subdomain edge} \\ & \text{or is a subdomain vertex,} \end{cases}$$

where

$$\mu_i := \min\{E_i/(1+\nu_i), E_j/(1+\nu_j)\}.$$

Here, i and j are the indices of the subdomains Ω_i and Ω_j which are related to the coupling constraint.

Using the projection $P^\top$, the determination of the Lagrangian multipliers $\underline{\lambda}$ and the determination of the constants $\underline{\gamma}$ of the system (4.23) can be separated, as $P^\top G\gamma = 0$. The solution $\underline{\lambda}$ of the system of linear equations

$$P^\top F\underline{\lambda} = P^\top \underline{d} \tag{4.25}$$

is computed by a projected parallelized conjugate gradient method, see, e.g., [14]. The initial guess is chosen as

$$\underline{\lambda}_0 = QG(G^\top QG)^{-1}\underline{e}$$

to satisfy the constraints (4.24). Then the constants $\underline{\gamma}$ of (4.23) can be computed by

$$\underline{\gamma} = (G^\top Q G)^{-1} G^\top Q(\underline{d} - F\underline{\lambda}). \tag{4.26}$$

Finally, the local solutions $\underline{u}_i$ of the representation (4.21) are computed.

As in the case of the standard BETI method, the condition number of the preconditioned all-floating BETI formulation (4.25) will be bounded independently of jumps in the coefficients, if the scaled hypersingular BETI preconditioner [16]

$$C_{\mathrm{BETI}}^{-1} = (BC_\beta^{-1}B^\top)^{-1} BC_\beta^{-1} D_{i,h} C_\beta^{-1} B^\top (BC_\beta^{-1}B^\top)^{-1} \tag{4.27}$$

is used. C_β^{-1} is a diagonal matrix which entries are defined by, see e.g. [11]

$$\left(C_\beta^{-1}\right)^{mn}[i,j] = \delta_{nm} \begin{cases} \frac{\sum_{\ell=1}^n \beta_\ell^\gamma}{\beta_i^\gamma} & \text{for } j = i, \\ 0 & \text{else,} \end{cases}$$

for $i, j = 1, \dots n$ and some parameter $\gamma \in [1/2, \infty)$. n denotes the number of subdomains adjacent to a global coupling nodes and $\beta_\ell = E_\ell/(1+\nu_\ell)$ are the related coefficients. The condition number of the all-floating method can be estimated like in the case of the standard FETI and BETI method [16].

Theorem 2 ([20])**.** *For the scaled hypersingular BETI preconditioner (4.27) and the projected all-floating BETI system (4.25), there holds the following estimate of the condition number*

$$\kappa(PC_{BETI}^{-1}P^\top F) \le c\left(1 + \log\frac{H}{h}\right)^2 \tag{4.28}$$

where the constant c is independent of h, H, the number p of subdomains and of the jumps of the values $E_i/(1+\nu_i)$. H denotes the maximum of the local diameters $H_i := diam\,\Omega_i$ of the subdomains and h the maximum of the meshsizes h_i of the subdomains Ω_i.

Proof. See [25]. □

For improved computational times, we reintroduce the local stresses

$$\underline{t}_i := V_{i,h}^{-1}(\frac{1}{2}M_{i,h} + K_{i,h})\underline{u}_i,$$

such that the system (4.18) is transformed into a two-fold saddle point problem

$$\begin{pmatrix} V_{1,h} & & & -\widehat{K}_{1,h} & & & \\ & \ddots & & & \ddots & & \\ & & V_{p,h} & & & -\widehat{K}_{p,h} & \\ \widehat{K}_{1,h}^\top & & & \widehat{D}_{1,h} & & & -\widetilde{B}_1^\top \\ & \ddots & & & \ddots & & \vdots \\ & & \widehat{K}_{p,h}^\top & & & \widehat{D}_{p,h} & -\widetilde{B}_p^\top \\ & & & \widetilde{B}_1 & \dots & \widetilde{B}_p & 0 \end{pmatrix} \begin{pmatrix} \underline{t}_1 \\ \vdots \\ \underline{t}_p \\ \underline{u}_1 \\ \vdots \\ \underline{u}_p \\ \underline{\lambda} \end{pmatrix} = \begin{pmatrix} \underline{0} \\ \vdots \\ \underline{0} \\ \underline{f}_{N,1} \\ \vdots \\ \underline{f}_{N,p} \\ \underline{b} \end{pmatrix}. \tag{4.29}$$

Here, the abbreviation

$$\widehat{K}_{i,h} = \frac{1}{2} M_{i,h} + K_{i,h}$$

is used. The two-fold saddle point problem (4.29) is solved by a preconditioned Bramble–Pasciak CG method [1] for two-fold saddle point problems including the projection P, see [14] for details. The involved preconditioners are an algebraic multigrid preconditioner [22] for the local single layer potentials V_i and the preconditioners (3.14) and (4.27) presented for the local Steklov–Poincaré operators S_i and the all-floating Schur complement system. All boundary integral operators are realized by the fast multipole method [8, 24].

Theorem 3. *Let the numbers of iterations of the algebraic multigrid preconditioner of the local single layer potentials V_i be bounded with respect to h. Then not more than $I(\varepsilon) = \mathcal{O}((1+\log(H/h))^1 \log \varepsilon^{-1})$ iterations and ops$(\varepsilon) = \mathcal{O}((H/h)^2(1+\log(H/h))^3 \log \varepsilon^{-1})$ arithmetical operations are required in order to reduce the initial error of the two-fold saddle point problem (4.29) by the factor $\varepsilon \in (0,1)$ in a parallel regime and the described manner. The number of iterations is robust with respect to the jumps in the coefficients. Moreover, not more than $\mathcal{O}((H/h)^2(1+\log(H/h))^2)$ storage units are needed per processor.*

Proof. The assertion follows from the spectral equivalence inequalities (3.12) and (4.27) and the complexity of $\mathcal{O}((H/h)^2(1+\log(H/h))^2)$ of the fast multipole realization [24] of the boundary integral operators. □

The standard BETI method requires $I(\varepsilon) = \mathcal{O}((1+\log(H/h))^2 \log \varepsilon^{-1})$ iterations and ops$(\varepsilon) = \mathcal{O}((H/h)^2(1+\log(H/h))^4 \log \varepsilon^{-1})$ arithmetical operations for the same setting. The all-floating version utilizes the improved condition number of the preconditioned local Steklov–Poincaré operators and shows a better asymptotic complexity.

5 Numerical Examples

The part of essential boundary conditions is in general relative small for problems in elasticity. Therefore a mixed boundary value problem of linear elastostatics is considered for a cube subdivided into eight subdomains with subdomain boundaries of 24 triangles each. We use the elasticity module $E = 200$ and the Poisson ratio $\nu = 0.3$ as material parameters. The upper and lower face of the cube define the Dirichlet part of the boundary. Neumann boundary conditions are predescribed on the remaining part of the boundary. The boundary data are given by the traces of a fundamental solution with a singularity outside the domain. The numbers of degrees of freedom for each formulation are given in Table 1. Each subdomain was refined up to five times. Finally, each subdomain boundary consists of 24576 triangles. The first column is the refinement level L and the second column describes the numbers for the primal system (2.4). Columns 6–8 give the numbers of unknowns of the all-floating BETI Schur complement system (4.22), its saddle point problem (4.18) and its two-fold saddle point problem (4.29), while columns 3–5 contain the corresponding numbers of the systems of the standard BETI method.

	DDD	B-Schur	B-SPP	B-2SPP	A-Schur	A-SPP	A-2SPP
L	(2.4)	(4.15)			(4.22)	(4.18)	(4.29)
0	111	105	321	897	225	561	1137
1	537	351	1239	3543	663	1863	4167
2	2397	1275	4947	14163	2259	6915	16131
3	10149	4851	19851	56715	8331	26811	63675
4	41781	18915	79611	227067	31995	105771	253227
5	169557	74691	318939	908763	125403	420363	1010187

Table 1: Numbers of degrees of freedom of the considered methods for 8 subcubes.

The system (2.4) of the primal Dirichlet domain decomposition method has more degrees of freedom than the Schur complement systems (4.15) and (4.22) of the BETI method and of the all-floating formulation. The numbers of degrees of freedom are larger for the all-floating formulation than for the standard BETI method due to the extra dual degrees of freedom at the Dirichlet part of the boundary.

	DDD (2.4)			B-2SPP			A-2SPP (4.29)		
L	t_1	t_2	It.	t_1	t_2	It.	t_1	t_2	It.
0	2	3	25(12)	2	4	77	3	4	63
1	4	14	60(15)	5	17	97	6	13	81
2	11	99	74(16)	11	97	106	12	76	80
3	30	575	85(16)	29	496	116	26	358	83
4	193	4128	92(16)	193	3699	131	157	2673	93
5	1353	37146	101(17)	1360	27531	150	1045	18935	102

Table 2: Comparison of the method for a mixed boundary value problem

In Table 2, the computational times and the numbers of iterations are compared for the primal Dirichlet domain decomposition method (2.4), the two-fold system of the BETI method and the two-fold system (4.29) of the all-floating formulation. All computations were executed on the cluster "mozart" of the Department of Simulation of Large Systems and the Chair of Numerics for Supercomputers at the University of Stuttgart. The Linux cluster consists of 64 nodes with 4 GB of RAM and 2 Intel Xeon processors with 3.066 GHz each. Each subdomain is assigned to a processor core. t_1 and t_2 are the computational times for setting up the system of linear equations and for solving this system, respectively. It denotes the number of iterations executed by a conjugate gradient method for a relative accuracy of $\varepsilon = 10^{-8}$. The approximation errors $\|u - u_h\|_{L_2(\Gamma)}$ of the Dirichlet data match each other very accurately. The all-floating formulation is the fastest of the three methods for this problem with mixed boundary conditions. In comparison to the standard

BETI method, the number of iterations and the computational times show the improved asymptotic complexity of the all-floating formulation. The reduced number of iterations is not only due to the improved preconditioning of the Steklov–Poincaré operators. Even the numbers of iterations of the Schur complement system (4.22) are smaller than in the case of the standard BETI method (4.15). For the fourth refinement level, the number of iterations is 33 instead of 38. For the finest refinement level, the all-floating method is about twice as fast as the primal Dirichlet domain decomposition method (2.4). In the case of a pure Dirichlet boundary value problem, the other methods might be faster for small problem sizes due to the small number of degrees of freedom. But the improved asymptotic complexity of the all-floating formulation pays off for large problem sizes anyway. In general, the numbers of iterations and the computational times of the all-floating BETI method seem to be almost independent of the distribution of the boundary conditions in contrast to the other two methods.

Next, a mixed boundary value problem of linear elastostatics with jumping coefficients is considered. The domain decomposition in Fig. 1 represents a piece of steel ($E = 210, \nu = 0.285$) by two subdomains surrounded by concrete ($E = 30, \nu = 0.17$). A total of 18 subdomains has been used. Each subdomain is discretized by a unit cube as before. The bottom side is fixed while a deformation is imposed on the top surface. The remaining part of the boundary has vanishing Neumann boundary conditions.

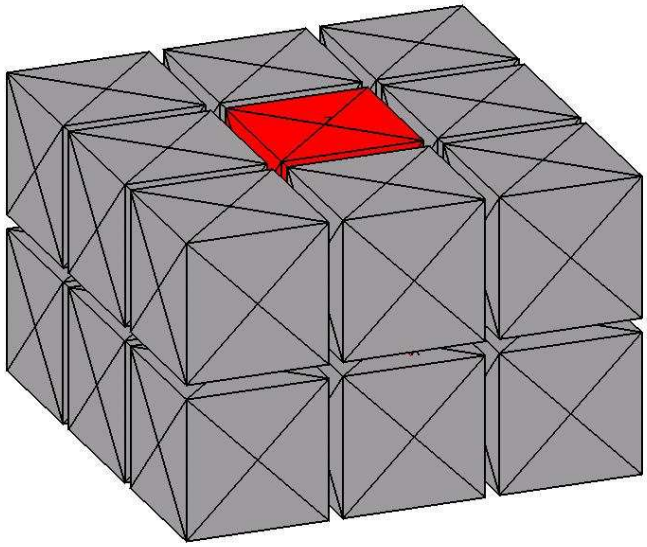

Figure 1: Domain decomposition of a piece of steel in concrete.

In the global refinement, each cube is refined up to 24576 boundary elements. A uniform extension of the surface mesh to the domain would consists of more than 14 million tetrahedrons for linear elastostatics. The numbers of degrees of freedom are listed in Table 3.

	DDD	B-Schur	B-SPP	B-2SPP	A-Schur	A-SPP	A-2SPP
L	(2.4)	(4.15)			(4.22)	(4.18)	(4.29)
0	219	267	753	2049	537	1293	2589
1	1071	927	2925	8109	1629	4329	9513
2	4827	3435	11697	32433	5649	16125	36861
3	20547	13203	46953	129897	21033	62613	145557
4	84819	51747	188313	520089	81177	247173	578949
5	344691	204867	754425	2081529	318969	982629	2309733

Table 3: Numbers of degrees of freedom for several methods for example of Fig. 1.

The computational times and the numbers of iterations are compared in Table 4 for the primal Dirichlet domain decomposition method (2.4), the BETI method and the all-floating two-fold formulation (4.29).

	Schur–CG (2.4)			BETI–SPP2			Allfl.–SPP2 (4.29)		
L	t_1	t_2	It.	t_1	t_2	It.	t_1	t_2	It.
0	5	7	53(10)	5	7	78	4	8	65
1	7	25	110(14)	7	19	100	7	19	82
2	13	181	130(14)	15	112	114	15	115	85
3	30	986	148(14)	30	562	129	27	476	95
4	191	6902	154(14)	189	4352	153	159	3119	105
5	1332	59264	166(16)	1334	31645	172	1060	23008	120

Table 4: Comparison of the methods for jumping coefficients

The BETI preconditioning technique performs well for jumping coefficients while the primal method (2.4) shows a rather large number of iterations. The numbers of iterations and the computational times are again smaller for the all-floating formulation than for the standard BETI method. The standard BETI method is about twice as fast as the primal method for the finest refinement level. The all-floating formulation is almost three times faster than the primal method. The improved asymptotic complexity of the BETI method and in particular of the all-floating formulation is indicated.

6 Conclusions

We presented the all-floating formulation of the BETI method for linear elasticity. The all-floating formulation simplifies the implementation of the methods, in particular in linear elasticity, and provides an improved asymptotic complexity compared to the standard version. The numerical examples are in agreement with the theoretical results.

Acknowledgement

This work has been supported by the German Research Foundation 'Deutsche Forschungsgemeinschaft (DFG)' under the grant SFB 404 'Multifield Problems in Continuum Mechanics', University of Stuttgart.

References

[1] J. H. Bramble and J. E. Pasciak. A preconditioning technique for indefinite systems resulting from mixed approximations of elliptic problems. *Math. Comput.*, 51(183):387–388, 1988.

[2] S. C. Brenner. An additive Schwarz preconditioner for the FETI method. *Numer. Math.*, 94(1):1–31, 2003.

[3] Z. Dostál, D. Horák, and R. Kučera. Total FETI—an easier implementable variant of the FETI method for numerical solution of elliptic PDE. *Comm. Numer. Methods Engrg.*, 22(12):1155–1162, 2006.

[4] C. Farhat, M. Lesoinne, P. LeTallec, K. Pierson, and D. Rixen. FETI-DP: A dual-primal unified FETI method. I: A faster alternative to the two-level FETI method. *Int. J. Numer. Methods Eng.*, 50(7):1523–1544, 2001.

[5] C. Farhat, M. Lesoinne, and K. Pierson. A scalable dual-primal domain decomposition method. *Numer. Linear Algebra Appl.*, 7(7-8):687–714, 2000.

[6] C. Farhat and F.-X. Roux. A method of finite element tearing and interconnecting and its parallel solution algorithm. *Int. J. Numer. Methods Eng.*, 32(6):1205–1227, 1991.

[7] C. Farhat and F.-X. Roux. Implicit parallel processing in structural mechanics. *Comput. Mech. Adv.*, 2(1):1–124, 1994.

[8] L. Greengard and V. Rokhlin. A fast algorithm for particle simulations. *J. Comput. Phys.*, 73:325–348, 1987.

[9] G. C. Hsiao, O. Steinbach, and W. L. Wendland. Domain decomposition methods via boundary integral equations. *J. Comput. Appl. Math.*, 125(1-2):521–537, 2000.

[10] G. C. Hsiao and W. L. Wendland. *Boundary integral equations*, volume 164 of *Applied Mathematical Sciences*. Springer-Verlag, Berlin, 2008.

[11] A. Klawonn and O. B. Widlund. FETI and Neumann-Neumann iterative substructuring methods: Connections and new results. *Commun. Pure Appl. Math.*, 54(1):57–90, 2001.

[12] A. Klawonn and O. B. Widlund. Selecting Constraints in Dual-Primal FETI Methods for Elasticity in Three Dimensions. In R. H. W. Hoppe, D. Keyes, J. Periaux, O. Pironneau, and J. Xu, editors, *Domain Decomposition Methods in Science and Engineering*, volume 40 of *Lect. Notes Comput. Sci. Eng.*, pages 67–81. Berlin: Springer, 2005.

[13] A. Klawonn and O. B. Widlund. Dual-primal FETI methods for linear elasticity. *Comm. Pure Appl. Math.*, 59(11):1523–1572, 2006.

[14] U. Langer, G. Of, O. Steinbach, and W. Zulehner. Inexact data-sparse boundary element tearing and interconnecting methods. *SIAM J. Sci. Comput.*, 29(1):290–314, 2007.

[15] U. Langer and C. Pechstein. All-floating coupled data-sparse boundary and interface-concentrated finite element tearing and interconnecting methods. *Comput. Vis. Sci.*, 11(4-6):307–317, 2008.

[16] U. Langer and O. Steinbach. Boundary element tearing and interconnecting methods. *Computing*, 71(3):205–228, 2003.

[17] U. Langer and O. Steinbach. Coupled boundary and finite element tearing and interconnecting methods. In R. Kornhuber et al., editor, *Domain decomposition methods in science and engineering. Selected papers of the 15th international conference on domain decomposition, Berlin, Germany, July 21-25, 2003. Lecture Notes in Computational Science and Engineering 40* , pages 83–97. Berlin: Springer, 2005.

[18] W. McLean. *Strongly elliptic systems and boundary integral equations.* Cambridge: Cambridge University Press, 2000.

[19] W. McLean and O. Steinbach. Boundary element preconditioners for a hypersingular integral equation on an interval. *Adv. Comput. Math.*, 11(4):271–286, 1999.

[20] G. Of. *BETI–Gebietszerlegungsmethoden mit schnellen Randelementverfahren und Anwendungen.* Doctoral thesis, Universtät Stuttgart, 2006.

[21] G. Of. The All-Floating BETI method: Numerical results. In U. Langer, M. Discacciati, D. Keyes, O. Widlund, and W. Zulehner, editors, *Domain Decomposition Methods in Science and Engineering XVII (2006)*, volume 60 of *Springer Lecture Notes in Computational Science and Engineering*, pages 295–302. Springer, Berlin, Heidelberg, 2008.

[22] G. Of. An efficient algebraic multigrid preconditioner for a fast multipole boundary element method. *Computing*, 82(2-3):139–155, 2008.

[23] G. Of and O. Steinbach. A fast multipole boundary element method for a modified hypersingular boundary integral equation. In W. Wendland et al., editor, *Analysis and*

simulation of multifield problems. Selected papers of the international conference on multifield problems, Stuttgart, Germany, April 8-10, 2002. Lect. Notes Appl. Comput. Mech. 12 , pages 163–169. Berlin: Springer, 2003.

[24] G. Of, O. Steinbach, and W. L. Wendland. Applications of a fast multipole Galerkin boundary element method in linear elastostatics. *Comput. Visual. Sci.*, 8:201–209, 2005.

[25] C. Pechstein. *Finite and Boundary Element Tearing and Interconnecting Methods for Multiscale Elliptic Partial Differential Equations*. PhD thesis, Johannes Kepler University Linz, 2008.

[26] S. Sauter and C. Schwab. *Randelementmethoden. Analyse, Numerik und Implementierung schneller Algorithmen*. Stuttgart: Teubner, 2004.

[27] O. Steinbach. *Stability estimates for hybrid coupled domain decomposition methods*. Lecture Notes in Mathematics 1809. Berlin: Springer, 2003.

[28] O. Steinbach. *Numerical Approximation Methods for Elliptic Boundary Value Problems. Finite and Boundary Elements*. Springer, New York, 2008.

[29] O. Steinbach and W. L. Wendland. The construction of some efficient preconditioners in the boundary element method. *Adv. Comput. Math.*, 9(1-2):191–216, 1998.

[30] A. Toselli and O. Widlund. *Domain decomposition methods—algorithms and theory*, volume 34 of *Springer Series in Computational Mathematics*. Springer-Verlag, Berlin, 2005.

Erschienene Preprints ab Nummer 2007/1

2007/1	M. Windisch: Modifizierte Randintegralgleichungen für elektromagnetische Streuprobleme.
2007/2	M. Kaltenbacher, G. Of, O. Steinbach: Fast Multipole Boundary Element Method for Electrostatic Field Computations.
2007/3	G. Of, A. Schwaigkofler, O. Steinbach: Boundary integral equation methods for inverse problems in electrical engineering.
2007/4	S. Engleder, O. Steinbach: Stabilized Boundary Element Methods for Exterior Helmholtz Problems.
2007/5	O. Steinbach, G. Unger: A Boundary Element Method for the Dirichlet Eigenvalue Problem of the Laplace Operator.
2007/6	O. Steinbach, M. Windisch: Modified combined field integral equations for electromagnetic scattering.
2007/7	S. Gemmrich, N. Nigam, O. Steinbach: Boundary Integral Equations for the Laplace–Beltrami Operator.
2007/8	G. Of: An efficient algebraic multigrid preconditioner for a fast multipole boundary element method.
2007/9	O. Steinbach (ed.): Jahresbericht 2006/2007.
2007/10	U. Langer, O. Steinbach, W. L. Wendland (eds.): 5th Workshop on Fast Boundary Element Methods in Industrial Applications, Book of Abstracts
2008/1	P. Urthaler: Schnelle Auswertung von Volumenpotentialen in der Randelementmethode.
2008/2	O. Steinbach (ed.): Workshop on Numerical Simulation of the Maxwell Equations. Book of Abstracts.
2008/3	G. Of, O. Steinbach, P. Urthaler: Fast Evaluation of Newton Potentials in the Boundary Element Method.
2008/4	U. Langer, O. Steinbach, W. L. Wendland (eds.): 6th Workshop on Fast Boundary Element Methods in Industrial Applications, Book of Abstracts.
2008/5	D. Brunner, G. Of, M. Junge, O. Steinbach, L. Gaul: A Fast BE-FE Coupling Scheme for Partly Immersed Bodies
2009/1	G. Of, T. X. Phan, O. Steinbach: An energy space finite element approach for elliptic Dirichlet boundary control problems.
2009/2	G. Of, T. X. Phan, O. Steinbach: Boundary element methods for Dirichlet boundary control problems.